International Journal of Latest Research in Engineering and Technology (IJLRET)
ISSN: 2454-5031
www.ijlret.com || Volume 06 - Issue 08 || August 2020 || PP. 31-44

Slope Stability Evaluation by Geo-mechanical and Kinematic analysis in 403 &403A km stretch between Vaiyampatty–Ayyalur Railway section, Dindigul, Tamil Nadu

Kathika Pavana Venkata Mani Kumar[1], Aravind S[1], Ramkumar K[1], Saranaathan, S.E[1]. Prasanna Venkatesh, S[2].
[1]*School of Civil Engineering, SASTRA Deemed University, Thanjavur – 613 401.*
[2]*Department of Applied Geology, School of Earth & Atmospheric Science, University of Madras, Chennai - 600025*

Abstract: The present study deals with assessment of stability in rock slopes using Geo-mechanical (RMR and SMR) and Kinematic technique. Attempt has been made to determine the class of instability using SMR method and determine factor of safety using planar and wedge technique. The present paper mainly explains the analysis of the instability of slope of railway cut slope present in 403 to 403A. Extensive field study was carried out to understand the behavior of rock mass. Laboratory experiments have been conducted to determine the various physical and mechanical properties of the rock mass. These properties have been used as input parameters for geo-mechanical and kinematic analysis. The possible failure modes were determined for the vulnerable slopes. In this study, analyses of rock slope stability were performed. The RMR result shows, 403/1, 403A/2 and 403/5 rock section depicts class III, III, and III respectively. As per Slope Mass Rating 403/1, 403A/2 and 403/5 come under partially stable condition, and 403/1- J3 comes under very unstable condition. The detailed Kinematic analysis carried out in 403/1 - J1, J2, 403A/2 - J2 and 403/5 – J2 for planar analysis and 403/1 – J1 – J2, 403/5 – J1 – J3, J2 – J3 and 403A/2 – J1 – J3, J2 – J3 are fulfil Hock and Bray wedge analysis. The Planar analysis shows 403/1 J3 and 403A/2 J2 are shows unsafe condition (FOS < 1) and 403/5 J2 and 403/1 J1 are safe (FOS > 1) in dry condition and unsafe in fully saturated condition. In Wedge analysis shows rock slopes 403/5 J1 – J3 is unsafe condition (FOS < 1) and other wedges are shows safe in condition (FOS > 1). The slope needs proper attention to minimize the regular and frequent failure every year mainly after the rainy season.

Keywords: Rock Mass Rating, Slope Mass Rating, Kinematic analysis, Planar and Wedge analysis. Factor of Safety (FOS).

I. Introduction

In the last few decades, there had been tremendous increase in the occurrence of natural disasters like Earthquakes, Landslides, Floods, Cyclones, Cloud burst, etc. Landslide is one of the disasters, which lead to a large-scale damage to properties and life. It frequently occurs in hilly regions like Himalaya, Western Ghats and Eastern Ghats. In Tamil Nadu, often landslides are seen in Blue Mountains, Kodaikanal, Yercaud and occasionally in the other areas. Vaiyampatty block is a revenue block in the Tiruchirappalli district of Tamil Nadu, India. There are many small temples in and around the village. Thekamalai is one of the most important hills situated near to Vaiyampatty. Popular tourist spot is Ponnaniyar dam which is situated 4km from Vaiyampatty. The first railway line in this region was open in 1857 connecting Madurai to Tiruchirappalli via Dindigul and onward. The newly laid track (BG) from Ayyalur to Vaiyampatty is for a length of 5.5 Kilometers cutting elevated rocky soil up to a depth of 100 feet. The old track length is about 3.8 km with a gradient of about 1 in 100 which was not suitable to operate trains with heavier loads at high speed. So when the gauge conversion project was taken up, this portion of track was diverted through longer length and the gradient was made as 1 in 200 which is suitable for trains with heavier loads and high speed. This was commissioned during 1999. The cut slope of the track is about 30m deep and more than 50 pair trains moving throughout the day. This is one of the reasons for high traffic intensity on the cut slope railway road led to numerous small landslides started in this section. In this context, this has been considered for slope stability analysis using geo-mechanical and kinematic analysis. The slope stability analyses of rock slopes have been carried out by various researchers [1], [2], [4], [3] and [5].

II. Study Area

Ayyalur-Vaiyampatty railway line is located between Panjamthangi and Mungil karai reserved forest hill area. This is one of the important railway networks in Southern Railway. The study area is surrounded by structural hill and constitutes a peneplain. The major soil types encountered in this area is loamy soil. The region is covered by Hornblende biotite gneiss with small patches of charnockite rocks. The railway section of 403 Km to 403A Km stone is found in Ayyalur - Vaimpatty revenue village. It is located between 10°29'52" and 10°29'27" N latitudes and 78°12'57" and 78°12'12" E longitudes. Three vulnerable slopes are selected for this study; it is clearly shown in Fig 1. In this surrounding railway section, the height varies from 312m to 394m above MSL. The study area falls under the Survey of India Topo sheets 58 J/2. The climate of this study area is a moderate one with a maximum and minimum temperature of 42°C and 25°C respectively. Winter seasons starts in the month of September and ends in December.

Fig 1. Location map of rock slopes

III. Local Geology

Crystalline rocks of Archaean to late Proterozoic age occupy over 80% of the area of the state, while the rest is covered by Phanerozoic sedimentary rocks mainly along the coastal belt and in a few inland River valleys. In this study area, the hard rock terrain comprises predominantly of Charnockite and Khondalite groups and their migmatitic derivatives, The Kadavur Anorthosite is distinctly post-tectonic rock type is located in northern part the study area.

IV. Methodology

4.1 Stereographic Analysis of Discontinuity

Stereographic analysis of the discontinuities has been carried out to know the probable modes of failure. In the present study only planar and wedge failures have been found. The field data for strike and dip of different structural discontinuity planes have been plotted and analyzed in the stereographic projection to analyze the role of various discontinuity planes for different types of failures. The poles of the discontinuity planes are contoured to find out different pole concentrations for defining the major discontinuity planes. The plane corresponding to the slope face has been also plotted on the same diagram. Fig 2 and 2A shows that few stereographic projections of the vulnerable slopes.

4.2 RMR and SMR Technique

Slope Mass Rating technique is a scheme of classification of slope stability for assessing instability in rock slopes. The technique as been developed by Romana [7] which is based on Rock Mass Rating (RMR) of Bieniawski [8] and the adjustment factor ratings for geological discontinuities and method of excavation of slopes. RMR is computed from the following five parameters:

- Strength of rock

- Rock Quality Designation (RQD)
- Spacing of discontinuities
- Condition of discontinuities
- Water inflow through discontinuities

Different ratings are given to these five parameters which are added to obtain the value of RMR (**Table1**). The SMR is expressed as:

SMR = RMR + (F1. F2. F3) + F4 (1)

Where,

F1 – refers to parallelism between strike of joints and slope face

F2 – refers to join dip amount or plunge of intersection of two joint planes in case of wedge slope.

F3 – refers to relationship between dip of joint or line of intersection of two joints and the dip of slope

F4 – refers to the adjustment factor of method of excavation. The ratings for these factors are given in **Table 2** and **Table 3**.

TABLE 2
SMR adjustment rating for joints

Case		Very Favorable	Favorable	Fair	Unfavorable	Very Unfavorable
P	$\lvert\alpha_j - \alpha_s\rvert$	>30°	30–20°	20–10°	10–5°	<5°
T	$\lvert\alpha_j - \alpha_s - 180°\rvert$					
P/T	F_1	0.15	0.40	0.70	0.85	1.00
P	$\lvert\beta_j\rvert$	<20°	20–30°	30–35°	35–45°	>45°
P	F_2	0.15	0.40	0.70	0.85	1.00
T	F_2	1	1	1	1	1
P	$\beta_j - \beta_s$	>10°	10–0°	0°	0°–(–10°)	<–10°
T	$\beta_j + \beta_s$	<110°	110–120°	>120°		
P/T	F_3	0	–6	–25	–50	–60

P = plane failure. α_s = slope dip direction. α_j = joint dip direction.
T = toppling failure. β_s = slope dip. β_j = joint dip.

Method	Natural Slope	Presplitting	Smooth Blasting	Regular Blasting	Deficient Blasting
F_4	+15	+10	+8	0	–8

$SMR = RMR - (F_1 \times F_2 \times F_3) + F_4$

Tentative Description of SMR Classes

Class No.	V	IV	III	II	I
SMR	0–20	21–40	41–60	61–80	81–100
Description	Very poor	Poor	Fair	Good	Very good
Stability	Very unstable	Unstable	Partially stable	Stable	Fully Stable
Failures	Large planar or soil-like	Planar or large wedges	Some joints or many wedges	Some blocks	None
Support	Reexcavation	Extensive corrective	Systematic	Occasional	None

TABLE 3
SMR adjustment rating for methods of excavation of slopes

Method	Natural Slope	Pre-splitting	Smooth Blasting	Blasting or Mechanical	Deficient Blasting
F4	+15	+10	+8	0	-8

4.3 Kinematic Technique

Kinematic analysis is a method used to analyze the potentiality of a rock slope for various modes of failures such as plane, wedge and toppling failures, which may occur due to the presence of unfavorably oriented discontinuities.

4.3.1 Planar failure

According to the Markland's test a slope has high probability of plane failure (Fig 3) if it satisfies $\psi s > \psi p > \phi$. The selected sections (3 Nos.) were studied in detail after collecting extensive field data. Factor of safety value for the slope is calculated as the ratio of total force resisting sliding to the total force to induce sliding. It is calculated by equation [6] as follows.

$$F = cA + (W.\cos\psi_p - U - V.\sin\psi_p) \tan\phi \; / \; W.\sin\psi_p + V.\cos\psi_p \qquad (2)$$

$$A = (H\text{-}z).\mathrm{cosec}\psi_p \qquad (3)$$

$$U = ½ \, \gamma_w.z_w. (H\text{-}z).\mathrm{cosec} \qquad (4)$$

$$V = ½ \, \gamma_w.z_w^{\,2} \qquad (5)$$

When the tension crack is on the upper surface

$$W = ½ \, \gamma.H^2 \{(1 - (z/H)^2) \cot\psi_p - \cot\psi_f\} \quad (6)$$

When the tension crack is on the slope face

$$W = ½ \, \gamma.H^2 \{(1 - (z/H)^2) \cot\psi_p . \; (\cot\psi_p.\tan\psi_f - 1)\} \; (7)$$

For the sake of simplicity, the equation can be rearranged in the form

$$F = (2c/\gamma H).P + \{Q.\cot\psi_p - R(P+S)\} \; / \; Q + R.S \cot\psi_p \; (8)$$

Where

$$P = (1 - z/H).\mathrm{cosec}\psi_p \qquad (9)$$

When the tension crack is on the upper surface

$$Q = \{(1 - (z/H)^2) \cot\psi_p - \cot\psi_f \} \sin\psi_p \qquad (10)$$

When the tension crack is on the slope

$$Q = \{(1 - (z/H)^2) \cot\psi_{p.} (\cot\psi_p. \tan\psi_f - 1) \qquad (11)$$

$$R = \gamma_w/\gamma. \; z_w/z \; . \; z/H \qquad (12)$$

$$S = z_w/z \; . \; z/H \; . \; \sin\psi_p \qquad (13)$$

Here P, Q, R and S are all dimensionless factors.

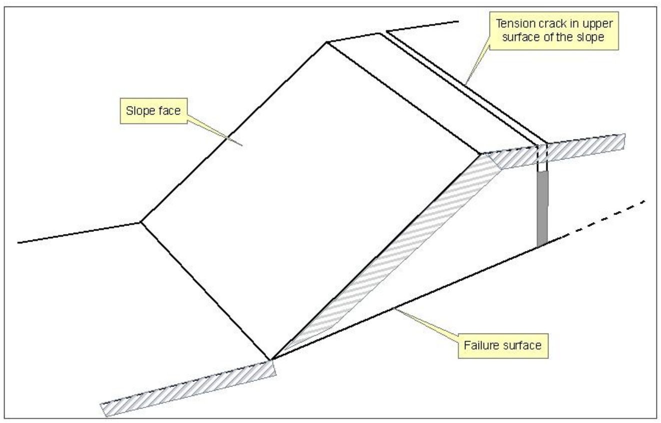

Fig 3. Geometry of slope with tension crack – Planar analysis

4.3.2 Wedge failure

It is concerned with the failure of slope in which structural features upon which sliding can occur strike across the slope crest and where sliding takes place along the line of intersection of two such planes is called Wedge failure. Fig 4 shows the geometry of the wedge which will be considered in the analysis. The water pressure distribution assumed for this analysis is based upon the hypothesis that the wedge itself is impermeable and that water enters the top of the wedge along lines of intersection 3 and 4 leaks from the slope face along lines of intersection 1 and 2.

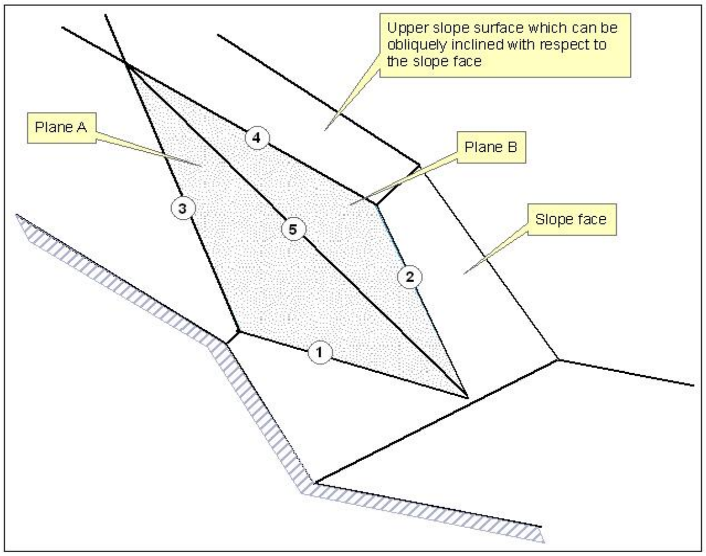

Fig 4. Geometry of wedge used for stability analysis

The numbering of the lines of intersection of the various planes involved in this problem is of extreme importance since total confusion can arise in the analysis if these numbers are mixed-up. The numbering used in stereo net is as follows. It is shown in Fig 5.

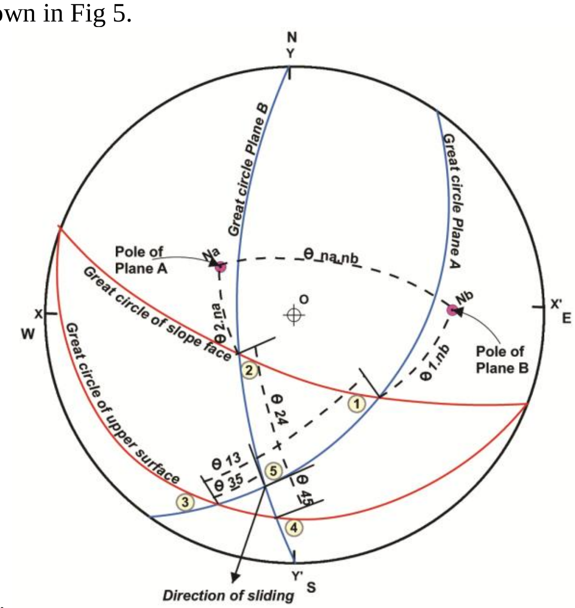

Fig 5. Stereo plot of data required for wedge stability analysis.

The factor of safety can be derived by using the following equation [6] for 3-D wedge stability analysis.

$$F = \{3/\gamma H\,(c_A.X + c_B.Y)\} + \{(A - (\gamma_w/2\gamma).X)\}\tan\phi_A + (B - (\gamma_w/2\gamma).Y)\tan\phi_B \qquad (14)$$

Where

c_A and c_B are the cohesive strengths of planes A and B
ϕ_A and ϕ_B are the angles of friction on plane A and B
γ is the density of the rock
γ_w is the density of the water
H is the total height of the wedge
X, Y, A and B are dimensionless factors which depend upon the geometry of the wedge.

$X = Sin\theta_{24} / Sin\theta_{45}.Cos_{2.na}$ (15)
$Y = Sin\theta_{13} / Sin\theta_{35}.Cos_{1.nb}$ (16)
$A = Cos\psi_a - Cos\psi_b.Cos\theta_{na.nb} / Sin\psi_5.Sin^2\theta_{na.nb}$ (17)
$B = Cos\psi_b - Cos\psi_a.Cos\theta_{na.nb} / Sin\psi_5.Sin^2\theta_{na.nb}$ (18)

Where ψ_a and ψ_b are the dips of planes A and B respectively and ψ_5 is the dip of intersection 5.

V. Result and Discussion

Based on rock mass rating parameters, RMR values have been obtained (**Table 4**). A perusal of the RMR values indicates that these values range from 51 to 53. The mode of slope failures calculated as among the attitude of joint plane and the slope. The assessment of slope has been carried out based on the values of SMR obtained for each zone. SMR values and the corresponding classes of instability of all the slopes are given in the **Table 5**. It has been found cut slopes coming under class V is the existing landslide slope while most of the joints under class III have shown minor failures.

TABLE 4
RMR and assessed classes of slopes

Sample location	Rock	Strength of intact Rock	RQD	Spacing of discontinuity	Conditions of discontinuity	Ground water conditions	RMR Value	Description	Class
403/1	Gneiss Rock	7	13	10	11	10	51	Fair	III
403A/2	Gneiss Rock	7	17	10	09	10	53	Fair	III
403/5	Gneiss Rock	7	17	8	11	10	53	Fair	III

According to Hock and Bray analysis slope has high probability of planar and wedge were studied in detail after collecting extensive field data. The descriptions of the individual sections are given in the following:

5.1 403/1 section

This rock slope section falls in 403/1 kilometer stone. The rocks are well exposed in the area. Highly fissile gneissic rock is present on this slope. The height of cut slope is about 9m. Three important joints J1, J2, and J3 are observed on the slope. A few bushes are present in this slope. The J1 and J2 joints are fulfill the Hock and Bray condition. In this analysis, the conditions of the slope are dry, 25%, 50% and fully saturated conditions and factor of safety was calculated by equation 2. Factor of safety of the joint J1 is 1.1002, 0.558, 0.476 and 0.455 for above said condition respectively. Factor of safety of the joint J2 is about 2.784, 0.750, 0.608 and 0584 for dry to fully saturated conation. In this section, the intersection of joint J1 – J2 performed the wedge condition. The intersection of plunge is about 38^o and N288^o direction. The calculation of Hock and Bray equation, factor of safety of plunge is about 3.084. It is safe in condition. The factor of safety was calculated and planar and wedge calculation was shown in **Table 6** and **Table 7** respectively.

5.2 403A/2 section

This slope section falls in near 403A/2 kilometer stone. The rocks are well outcropped in this area. It is highly joined in nature. Quartz veins are occurs in this section. The height of cut slope is about 12m. Bushes and grass are seen this slope. In this section also three joint systems are identified (J1, J2 and J3). The factor of safety was calculated as per Hock and Bray condition. Joint J2 is fulfilling planar condition. In this analysis, the condition of the slope are dry, one forth, half and fully saturated condition. Factor of safety of the J2 are 0.762, 0.4895, 0.4390 and 0.4240 for above said conditions. In this section, two wedges are identified as J1 – J3 and J2 – J3 and intersection of wedges are 12° and N28° and 38° and N40° respectively. The calculation of Hock and Bray equation, factor of safety of J1 – J3 and J2 – J3 is about 5.099 and 1.3057 respectively. **Table 6** and **Table 7** are shown the planar and wedge calculation.

5.3 403/5 section

In this slope highly fissile rocks are well exposed. The slope has slide in last year monsoon. The height of the slope is about 11.5m. Three joint sets are well exposed. This is the section also fulfilling the Hock and Bray planar and wedge conditions. The factor of safety was calculated and tabulated. Joint J2 is fulfilling the Hock and Bray condition for planar analysis. As per the analysis, factor of safety of the slope is 3.98 for dry condition and 0.6793 for fully saturated condition. Intersection of Joints J1 – J3 and J2 – J3 performed the wedge condition. As per wedge calculation, factor of safety of J1 – J3 and J2 – J3 are less than one. It is shown in **Table 6** and **Table 7**.

VI. Conclusion

The present study of slope stability assessment based on Slope Mass Rating technique has classified the slopes into five classes of instability. The study as revealed that the orientation of discontinuities in relation to slope is a very important parameter for assessing the stability. As per SMR analysis, three slopes are coming under partially stable to unstable conditions. Kinematic analysis of the slopes indicates that planar and wedge failure modes are detected in these slopes. All three slopes are fulfills planar and wedge analysis. As per planar analysis, the section 403/1, 403/5 and 40A/2 are safe in dry condition and unsafe in fully saturated condition. Due to wedge analysis, 4031, 403/5 and 403A/2 are safe in all condition. But wedge J1 – J3 in 403/5 section unsafe in all condition.

References

[1]. Sharma RK, Mehta BS, Jamwal CS (2013) *"*Cut slope stability evaluation of NH-21 along Natayan–Gambhrola section, Bilaspur district, Himachal Pradesh, India*", Nat Hazards 66, 249–270. doi:10.1007/s11069-012-0469-x*

[2]. Singh TN, Singh R, Singh B, Sharma LK, Singh R, Ansari MK (2016) "Investigations and stability analyses of Malin village landslide of Pune district, Maharashtra, India", *Nat Hazards* 81(3), 2019–2030. doi:10.1007/s11069-016-2241-0

[3]. Saranaathan.S E., and Kannan.M., "SMR and Kinematic Analysis for slope stability along Bodi- Bodimettu Ghat section, Tamil Nadu", *Journal of Geological Society of India*, 89, 589 - 599, 2017.

[4]. S.Anabalangan, V. Ramesh, and S.E.Saranaathan "Cut slope stability assessment along ghat road section of Kolli Hills, India", *Natural Hazard*, 86, 1081 - 1104, 2017.

[5]. Pulicherla Naga Vinay, S.Prasanna Venkatesh, and S.E. Saranaathan, "Geomechanical Analysis of Recent (2017) rock fall in Tirupati – Tirumala Ghat section II near 9th Mile stone, Tirupati, Anadhra Pradesh, India", *International Journal of Earth Science and Engineering*, 11(4), 281 – 287, 2018.

[6]. Hoek E, Bray JW (1981) "Rock slope engineering". Stephen Austin and Sons Limited Publishers, Hertford.

[7]. Romana.M "New adjustment ratings for application of Bieniawski classification to slopes". Proceedings of the international symposium on the role of rock mechanics in excavations for mining and civil works. *International society of rock mechanics, Zacatecas*, 49–53, 1985.

[8]. Bieniawski ZT The "Geomechanics classification in rock engineering applications". In: *Proceedings of the 4th international congress rock mechanics*, Montreux, Balkema, Rotterdam, 2. 41–48, 1979

TABLE 5
SMR and assessed instability classes of slopes

Slope	Joint	RMR	Rating for adjustment factors F1	F2	F3	F4	SMR	Class	Stability
403/1	J1	51	0.4	0.85	-50	0	34	III	Partially Stable
	J2		0.4	0.7	-6	0	49.32	III	Partially Stable
	J3		0.7	1.0	-60	0	9	V	Very Unstable
	J1 –J3		0.7	1.0	-6	0	51	III	Partially Stable
403/5	J2	53	0.4	0.7	0	0	55	III	Partially Stable
	J1 – J3		0.7	1.0	0	0	53	III	Partially Stable
	J2 – J3		0.15	1.0	0	0	53	III	Partially Stable
403A/2	J2	53	1.0	0.85	0	0	55	III	Partially Stable
	J1 – J3		0.7	0.4	-6	0	53.32	III	Partially Stable
	J2 – J3		0.15	0.85	-50	0	48.62	III	Partially Stable

A. CLASSIFICATION PARAMETERS AND THEIR RATINGS									
Parameter			Range of values						
1	Strength of intact material	Point - load strength index	> 10 MPa	4 - 10 MPa	2 - 4 MPa	1 - 2 MPa	For this low range - uniaxial compressive test is preferred		
		Uniaxial comp. strength	> 250 MPa	100 - 250 MPa	50 - 100 MPa	25 - 50 MPa	5 - 25 MPa	1 - 5 MPa	<1 MPa
	Rating		15	12	7	4	2	1	0
2	Drill core Quality RQD		90%-100%	75%-90%	50%-75%	25%-50%	< 25%		
	Rating		20	17	13	8	3		
3	Spacing of discontinuities		>2m	0.6-2m	200-600mm	60-200mm	< 60mm		
	Rating								
4	Condition of discontinuities		Very rough surfaces Not continuous No separation Unweathered rock	Slightly rough surfaces Separation < 1 mm Slightly weathered	Slightly rough surfaces Separation < 1 mm Hightly weathered	Slicknesided surfaces or Gauge < 5 mm thick or Separation 1-5 mm Continuous	Soft gauge > 5 mm thick or Separation > 5 mm Continuous		
	Rating		30	25	20	10	0		
5	Ground water	Inflow per 10m tunnel length (l/m)	None	< 10	10 to 25	25 to 125	> 125		
		(Joint water press)/(Major principal σ	0	< 0.1	0.1 to 0.2	0.2 to 0.5	> 0.5		
		General conditions	Complrtly dry	Damp	Wet	Dripping	Flowing		
	Rating		15	10	7	4	0		
B. ROCK MASS CLASSES DETERMINED FROM TOTAL RATINGS									
Rating			100 - 81	80 - 61	60 - 41	40 - 21	< 21		
Class number			I	II	III	IV	V		
Description			Very good rock	Good rock	Fair rock	Poor rock	Very poor rock		
C. MEANING OF ROCK CLASSES									
Class number			I	II	III	IV	V		
Average stand-up time			20 yrs for 15 span	1 year for 10m span	1 week for 5m span	10 hrs for 2.5m span	30 min for 1m span		
Cohesion of rock mass (kPa)			> 400	300 - 400	200 - 300	100 - 200	< 100		
Friction angle of rock mass (deg)			> 45	35 - 45	25 - 35	15 - 25	< 15		

Table 1. Rock Mass Rating (Bieniawski 1989)

TABLE 6
Planar calculation

Section ID	Input Data	Function value	Calculations using formula	Results
403/1 J1	$\psi_p = 43°$ $\psi_f = 39°$ γ = 2.368gm/cc γ_w = 1gm/cc z_w = 9m z = 9m c = 938.13gm/cc H = 9m	Cosecψ_p = 1.468 Cotψ_p = 1.072 Cotψ_f = 1.236 Sinψ_p = 0.681 γ_w/γ = 0.422 z_w/z = 1.0;0.5;0.25;0 z/H = 1.0000 2c/γH = 4.504	P = (1– z/H).cosecψ_p = [(1-9/9)].cosec 43 = 0	P = 0
			Q = {(1– (z/H)^2) cotψ_p – cotψ_f } sinψ_p = 0- 1.23 ×0.6819 = -0.842	Q = -0.842
			When, zw/z = 1; R = γ_w/γ. z_w/z . z/H = 0.48	R=0.48 R= 0.24 R=0.10 R=0
			When, zw/z = 0.5; R= γ_w/γ. z_w/z . z/H = 024	
			When, zw/z = 0.25;R= γ_w/γ. z_w/z . z/H = 0.10	
			When, zw/z = 0; R = γ_w/γ. z_w/z . z/H = 0	
			When zw/z = 1; S = z_w/z . z/H . sinψp = 0.788	S = 0.707 S =0.0.35 S =0.176 S =0
			When zw/z = 0.5; S = z_w/z . z/H . sinψp = 0.394	
			When zw/z =0.25; S = z_w/z . z/H . sinψp =0.197	
			When zw/z = 0; S = z_w/z . z/H . sinψp = 0	
Case 1 : when zw/z = 1, i.e : When tension crack is completely filled with water (Zw=Z), FoS = 1.1002				
Case 2 : when zw/z = 0.5, i.e.: When the tension crack is filled with 50% of water, FOS = 0.558				
Case 3 : when zw/z = 0.25, i.e.: when the tension crack is filled with 25% of water, FOS = 0.476				
Case 4 : when zw/z = 0, i.e.: when the tension crack is dry, FOS = 0.455				

Section ID	Input Data	Function value	Calculations using formula	Results
403/1 J2	$\psi_p = 36°$ $\psi_f = 39°$ γ = 2.368gm/cc γ_w = 1gm/cc z_w = 9m z =9m c = 938.13gm/cc H = 9m	Cosecψ_p = 1.703 Cotψ_p = 1.377 Cotψ_f = 0.1.236 Sinψ_p = 0.5877 γ_w/γ = 0.422 z_w/z = 1.0;0.5;0.25;0 z/H = 1.0000 2c/γH = 4.504	P = (1– z/H).cosecψ_p = [1-(9/9)]= 0	P = 0
			Q = {(1– (z/H)^2) cotψ_p – cotψ_f } sinψ_p = -1.234 × 0.587 = -0.724	Q = -0.724
			When, zw/z = 1; R = γ_w/γ. z_w/z . z/H = 0.48	R=0.48 R= 0.24 R=0.10 R=0
			When, zw/z = 0.5; R= γ_w/γ. z_w/z . z/H = 0.24	
			When, zw/z = 0.25;R= γ_w/γ. z_w/z . z/H = 0.10	
			When, zw/z = 0; R = γ_w/γ. z_w/z . z/H = 0	
			When zw/z = 1; S = z_w/z . z/H . sinψp = 0.587	S = 0.587 S =0.293 S =0.146 S =0
			When zw/z = 0.5; S = z_w/z . z/H . sinψp = 0.293	
			When zw/z =0.25; S = z_w/z . z/H . sinψp =0.146	
			When zw/z = 0; S = z_w/z . z/H . sinψp = 0	
Case 1 : when zw/z = 1, i.e : When tension crack is completely filled with water (Zw=Z), FoS = 2.784				
Case 2 : when zw/z = 0.5, i.e.: When the tension crack is filled with 50% of water, FOS = 0.750				
Case 3 : when zw/z = 0.25, i.e.: when the tension crack is filled with 25% of water, FOS = 0.608				
Case 4 : when zw/z = 0, i.e. : when the tension crack is dry, FOS = 0.584				

Section ID	Input Data	Function value	Calculations using formula	Results
403/1 J3	$\psi_p = 82°$ $\psi_f = 39°$ γ = 2.368gm/cc γ_w = 1gm/cc z_w = 9m z = 9m c = 938.13gm/cc H = 9m	Cosecψ_p = 1.0101 Cotψ_p = 0.140 Cotψ_f = 1.236 Sinψ_p = 0.99 γ_w/γ = 0.422 z_w/z = 1.0;0.5;0.25;0 z/H = 1.0000 2c/γH = 4.504	P = (1– z/H).cosecψ_p = [1-(9/9)]cosec 82 = 0	P = 0
			Q = {(1– (z/H)^2) cotψ_p – cotψ_f } sinψ_p = (-1.0943)*0.990 = -1.0833	Q =-1.0833
			When, zw/z = 1; R = γ_w/γ. z_w/z . z/H = 104223	R=0.4223 R= 0.2111 R=0.1055 R=0
			When, zw/z = 0.5; R= γ_w/γ. z_w/z . z/H = 0.2111	
			When, zw/z = 0.25;R= γ_w/γ. z_w/z . z/H = 0.1055	
			When, zw/z = 0; R = γ_w/γ. z_w/z . z/H = 0	
			When zw/z = 1; S = z_w/z . z/H . sinψp = 0.9902	S = 0.9902 S =0.4951 S =0.2475 S =0
			When zw/z = 0.5; S = z_w/z . z/H . sinψp = 0.4951	
			When zw/z =0.25; S = z_w/z . z/H . sinψp =0.2475	
			When zw/z = 0; S = z_w/z . z/H . sinψp = 0	
Case 1 : when zw/z = 1, i.e : When tension crack is completely filled with water (Zw=Z), FoS = 0.23				
Case 2 : when zw/z = 0.5, i.e.: When the tension crack is filled with 50% of water, FOS = 0.10				
Case 3 : when zw/z = 0.25, i.e.: when the tension crack is filled with 25% of water, FOS = 0.067				
Case 4 : when zw/z = 0, i.e. : when the tension crack is dry, FOS = 0.05962				

Section ID	Input Data	Function value	Calculations using formula	Results
403/5J2	$\psi_p = 32°$ $\psi_f = 49°$ γ = 2.368gm/cc γ_w = 1gm/cc z_w = 11.5 cm z = 11.5m c = 938.13gm/cc H = 11.5m	Cosecψ_p = 1.92 Cotψ_p = 1.61 Cotψ_f = 0.86 Sinψ_p = 0.529 γ_w/γ = 0.422 z_w/z = 1.0;0.5;0.25;0 z/H = 1.0000 2c/γH = 4.504	P = (1– z/H).cosecψ_p = 0	P = 0
			Q = {(1– (z/H)^2) cotψ_p – cotψ_f } sinψ_p = [(1-1^{2}cot 32-cot 49)] = -0.4606	Q =-0.4606
			When, zw/z = 1; R = γ_w/γ. z_w/z . z/H = 0.4223	R=0.4223 R= 0.2115 R=0.1057 R=0
			When, zw/z = 0.5; R= γ_w/γ. z_w/z . z/H = 0.2115	
			When, zw/z = 0.25;R= γ_w/γ. z_w/z . z/H = 0.1057	
			When, zw/z = 0; R = γ_w/γ. z_w/z . z/H = 0	
			When zw/z = 1; S = z_w/z . z/H . sinψp = 0.5299	S = 0.5299 S =0.265 S =0.1325 S =0
			When zw/z = 0.5; S = z_w/z . z/H . sinψp = 0.265	
			When zw/z =0.25; S = z_w/z . z/H . sinψp =0.1325	
			When zw/z = 0; S = z_w/z . z/H . sinψp = 0	
Case 1 : when zw/z = 1, i.e : When tension crack is completely filled with water (Zw=Z), FOS = 3.98				
Case 2 : when zw/z = 0.5, i.e.: When the tension crack is filled with 50% of water, FOS = 2.744				
Case 3 : when zw/z = 0.25, i.e.: when the tension crack is filled with 25% of water, FOS = 0.7279				
Case 4 : when zw/z = 0, i.e. : when the tension crack is dry, FOS = 0.6793				

Section ID	Input Data	Function value	Calculations using formula	Results
403A/2 J2	$\psi_p = 45°$ $\psi_f = 34°$ γ = 2.368gm/cc γ_w = 1gm/cc z_w = 12m z = 12m c = 938.13gm/cc H = 12m	Cosecψ_p = 1.41 Cotψ_p = 1 Cotψ_f =1.03 Sinψ_p = 0.707 γ_w/γ = 0.422 z_w/z = 1.0;0.5;0.25;0 z/H = 1.0000 $2c/\gamma H$ =4.504	P = (1– z/H).cosecψ_p = [1-(12/12)cosec45= 0	P = 0
			Q = {(1– (z/H)^2) cotψ_p – cotψ_f } sinψ_p = -1.4825 × 0.7071 = -1.04828	Q = 0.6611
			When, zw/z = 1; R = γ_w/γ. z_w/z . z/H = 1.66	R=0.4221 R= 0.211 R=0.1055 R=0
			When, zw/z = 0.5; R= γ_w/γ. z_w/z . z/H = 0.1835	
			When, zw/z = 0.25;R= γ_w/γ. z_w/z . z/H = 0.09175	
			When, zw/z = 0; R = γ_w/γ. z_w/z . z/H = 0	
			When zw/z = 1; S = z_w/z . z/H . sinψp = 0.788	S = 0.1767 S =0.3535 S =0.707 S =0
			When zw/z = 0.5; S = z_w/z . z/H . sinψp = 0.394	
			When zw/z =0.25; S = z_w/z . z/H . sinψp =0.197	
			When zw/z = 0; S = z_w/z . z/H . sinψp = 0	
Case 1 : when zw/z = 1, i.e : When tension crack is completely filled with water (Zw=Z), FoS = 0.7622				
Case 2 : when zw/z = 0.5, i.e.: When the tension crack is filled with 50% of water, FOS = 0.48955				
Case 3 : when zw/z = 0.25, i.e.: when the tension crack is filled with 25% of water, FOS = 0.43900				
Case 4 : when zw/z = 0, i.e. : when the tension crack is dry, FOS = 0.4240				

TABLE 7
Wedge calculation

Section ID	Input Data	Function value	Calculations using formula	Results
403/1 J1-J2	ψ_a = 43° ψ_b = 36° ψ_5 = 38° $\theta_{na.nb}$ = 34°	$Cos\psi_a$ = 0.7313 $Cos\psi_b$ = 0.8090 $Sin\psi_5$ = 0.6156 $Cos\theta_{na.nb}$ = 0.8290 $Sin^2\theta_{na.nb}$ = 0.3216	$A = Cos\psi_a - Cos\psi_b.Cos\theta_{na.nb} / Sin\psi_5.Sin^2\theta_{na.nb}$ = 0.0607 / 0.1927= 0.3151 $B = Cos\psi_b - Cos\psi_a.Cos\theta_{na.nb} / Sin\psi_5.Sin^2\theta_{na.nb}$ = 0.2027/ 0.1926 = 1.0524	A = 0.3151 B = 1.0524
	θ_{24} = 86° θ_{45} = 76° θ_{2na} = 84°	$Sin\theta_{24}$ = 0.9975 $Sin\theta_{45}$ = 0.9702 $Cos\theta_{2na}$ = 0.0697	$X = Sin\theta_{24} / Sin\theta_{45}.Cos_{2.na}$ = 0.9975 / 0.9004 = 1.1077	X = 1.1077
	θ_{13} = 56° θ_{35} = 48° θ_{1nb} = 86°	$Sin\theta_{13}$ = 0.8290 $Sin\theta_{35}$ = 0.7431 $Cos\theta_{1nb}$ = 0.0697	$Y = Sin\theta_{13} / Sin\theta_{35}.Cos_{1.nb}$ = 0.8290/ 0.6734 = 1.2310	Y = 1.2310
	ϕ_A = 23° ϕ_B = 23° γ = 2.368g/cm^2 γ_w = 1g/ cm^3 c_A = 938.13g/cm^2 c_B = 938.13g/ cm^2 H = 900cm	$Tan\phi_A$ = 0.4244 $Tan\ \phi_B$ = 0.4244 $3/\gamma H$ =0.001407	$F = \{3/\gamma H (c_A.X + c_B.Y)\} + \{(A – (\gamma_w/2\gamma).X) \}tan\phi_A + (B – (\gamma_w/2\gamma).Y) tan\phi_B$ = 3.6338 - 0.002673 + 0.3363	F = 3.087
403/5 J1-J3	ψ_a = 20° ψ_b = 43° ψ_5 = 8° $\theta_{na.nb}$ = 62°	$Cos\psi_a$ = 0.9396 $Cos\psi_b$ = 0.7313 $Sin\psi_5$ = 0.1391 $Cos\theta_{na.nb}$ = 0.4694 $Sin^2\theta_{na.nb}$ = 0.7795	$A = Cos\psi_a - Cos\psi_b.Cos\theta_{na.nb} / Sin\psi_5.Sin^2\theta_{na.nb}$ = 0.5963/0.1084 = 5.5011 $B = Cos\psi_b - Cos\psi_a.Cos\theta_{na.nb} / Sin\psi_5.Sin^2\theta_{na.nb}$ = 0.2902 / 0.1084 = 2.676	A =5.5011 B = 2.676
	θ_{24} = 41° θ_{45} = 4° θ_{2na} = 50°	$Sin\theta_{24}$ = 0.6946 $Sin\theta_{45}$ = 0.0697 $Cos\theta_{2na}$ = 0.6427	$X = Sin\theta_{24} / Sin\theta_{45}.Cos_{2.na}$ = 0.6946/-0.573 = -1.212	X = -1.212
	θ_{13} = 86° θ_{35} = 12° θ_{1nb} = 30°	$Sin\theta_{13}$ = 0.9975 $Sin\theta_{35}$ = 0.2079 $Cos\theta_{1nb}$ = 0.8660	$Y = Sin\theta_{13} / Sin\theta_{35}.Cos_{1.nb}$ = 0.9975/-0.6581 = -1.5157	Y = -1.5157
	ϕ_A = 23° ϕ_B = 23° γ = 2.368g/cm^2 γ_w = 1g/ cm^3 c_A = 938.13g/cm^2 c_B = 938.13g/ cm^2 H = 1150cm	$Tan\phi_A$ = 0.4244 $Tan\ \phi_B$ = 0.4244 $3/\gamma H$ =0.0011016	$F = \{3/\gamma H (c_A.X + c_B.Y)\} + \{(A – (\gamma_w/2\gamma).X) \}tan\phi_A + (B – (\gamma_w/2\gamma).Y) tan\phi_B$ = -2.8691+2.45+1.266	F = 0.83
403/5 J2-J3	ψ_a = 32° ψ_b = 43° ψ_5 = 18° $\theta_{na.nb}$ = 70°	$Cos\psi_a$ = 0.8480 $Cos\psi_b$ = 0.7313 $Sin\psi_5$ = 0.3090 $Cos\theta_{na.nb}$ = 0.3420 $Sin^2\theta_{na.nb}$ = 0.8830	$A = Cos\psi_a - Cos\psi_b.Cos\theta_{na.nb} / Sin\psi_5.Sin^2\theta_{na.nb}$ = 0.5979/0.2728 = 2.1917 $B = Cos\psi_b - Cos\psi_a.Cos\theta_{na.nb} / Sin\psi_5.Sin^2\theta_{na.nb}$ = 0.4412/0.2728 = 1.6176	A = 2.1917 B = 1.6176
	θ_{24} = 34° θ_{45} = 12° θ_{2na} = 64°	$Sin\theta_{24}$ = 0.5591 $Sin\theta_{45}$ = 0.2079 $Cos\theta_{2na}$ = 0.4683	$X = Sin\theta_{24} / Sin\theta_{45}.Cos_{2.na}$ = 0.5591/-0.2304 = -2.4266	X = -2.4266
	θ_{13} = 108° θ_{35} = 20° θ_{1nb} = 22°	$Sin\theta_{13}$ = 0.9510 $Sin\theta_{35}$ = 0.3420 $Cos\theta_{1nb}$ = 0.9271	$Y = Sin\theta_{13} / Sin\theta_{35}.Cos_{1.nb}$ = 0.9510/-0.5851 = -1.6253	Y = -1.6253
	ϕ_A = 23° ϕ_B = 23°	$Tan\phi_A$ = 0.4244 $Tan\ \phi_B$ = 0.4244	$F = \{3/\gamma H (c_A.X + c_B.Y)\} + \{(A – (\gamma_w/2\gamma).X) \}tan\phi_A + (B – (\gamma_w/2\gamma).Y) tan\phi_B$	F = -2.198

	γ = 2.368g/cm^2 γ_w = 1g/ cm^3 c_A = 938.13g/cm^2 c_B = 938.13g/ cm^2 H = 900cm	$3/\gamma H$ =0.001407	= -4.1851+0.7127+1.2744	
403A/ 2 J1-J3	ψ_a = 53° ψ_b = 46° ψ_5 = 28° $\theta_{na.nb}$ = 88°	$\text{Cos}\psi_a$ = 0.6018 $\text{Cos}\psi_b$ = 0.6946 $\text{Sin}\psi_5$ = 0.4694 $\text{Cos}\theta_{na.nb}$ = 0.0348 $\text{Sin}^2\theta_{na.nb}$ = 0.9987	A = $\text{Cos}\psi_a$ - $\text{Cos}\psi_b.\text{Cos}\theta_{na.nb}$ / $\text{Sin}\psi_5.\text{Sin}^2\theta_{na.nb}$ = 0.577 6/0.4687 = 1.2321 B = $\text{Cos}\psi_b$ - $\text{Cos}\psi_a.\text{Cos}\theta_{na.nb}$ / $\text{Sin}\psi_5.\text{Sin}^2\theta_{na.nb}$ = 0.6736/0.4687 = 1.4372	A = 1.2321 B = 1.4372
	θ_{24} = 32° θ_{45} = 24° θ_{2na} = 90°	$\text{Sin}\theta_{24}$ = 0.500 $\text{Sin}\theta_{45}$ = 0.4067 $\text{Cos}\theta_{2na}$ = 0	X = $\text{Sin}\theta_{24}$ / $\text{Sin}\theta_{45}.\text{Cos}_{2.na}$ = 0.5000/0.4067 = -12.32	X = 1.2294
	θ_{13} = 32° θ_{35} = 22° θ_{1nb} = 78°	$\text{Sin}\theta_{13}$ = 0.5299 $\text{Sin}\theta_{35}$ = 0.3746 $\text{Cos}\theta_{1nb}$ = 0.2079	Y = $\text{Sin}\theta_{13}$ / $\text{Sin}\theta_{35}.\text{Cos}_{1.nb}$ = 0.5299/0.3746= 3.178	Y = 3.178
	ϕ_A = 23° ϕ_B = 23° γ = 2.368g/cm^2 γ_w = 1g/ cm^3 c_A = 938.13g/cm^2 c_B = 938.13g/ cm^2 H = 1200cm	$\text{Tan}\phi_A$ = 0.4245 $\text{Tan}\ \phi_B$ = 0.4245 $3/\gamma H$ =0.001055	F = {$3/\gamma H$ (c_A.X + c_B.Y)} + {(A – ($\gamma_w/2\gamma$).X) }$\tan\phi_A$ + (B – ($\gamma_w/2\gamma$).Y) $\tan\phi_B$ = 4.362+0.4127+0.3254	F = 5.099
403A//2 J2-J3	ψ_a = 45° ψ_b = 46° ψ_5 = 40° $\theta_{na.nb}$ = 52°	$\text{Cos}\psi_a$ = 0.7071 $\text{Cos}\psi_b$ = 0.6946 $\text{Sin}\psi_5$ = 0.6427 $\text{Cos}\theta_{na.nb}$ = 0.6516 $\text{Sin}^2\theta_{na.nb}$ = 0.6209	A = $\text{Cos}\psi_a$ - $\text{Cos}\psi_b.\text{Cos}\theta_{na.nb}$ / $\text{Sin}\psi_5.\text{Sin}^2\theta_{na.nb}$ = 0.2795/0.3990 = 0.7004 B = $\text{Cos}\psi_b$ - $\text{Cos}\psi_a.\text{Cos}\theta_{na.nb}$ / $\text{Sin}\psi_5.\text{Sin}^2\theta_{na.nb}$ = 0.1843/0.3990 = 0.4619	A = 0.7004 B = 0.4619
	θ_{24} = 32° θ_{45} = 46° θ_{2na} = 90°	$\text{Sin}\theta_{24}$ = 0. 5299 $\text{Sin}\theta_{45}$ = 0.7193 $\text{Cos}\theta_{2na}$ = 0	X = $\text{Sin}\theta_{24}$ / $\text{Sin}\theta_{45}.\text{Cos}_{2.na}$ = 0.5/0.7193 = 0.7366	X = 0.7366
	θ_{13} = 176° θ_{35} = 60° θ_{1nb} = 92°	$\text{Sin}\theta_{13}$ = 0.0697 $\text{Sin}\theta_{35}$ = 0.8660 $\text{Cos}\theta_{1nb}$ = -0.0348	Y = $\text{Sin}\theta_{13}$ / $\text{Sin}\theta_{35}.\text{Cos}_{1.nb}$ = 0.0697/0.9008 = 0.0773	Y = 0.0773
	ϕ_A = 23° ϕ_B = 23° γ = 2.368g/cm^2 γ_w = 1g/ cm^3 c_A = 938.13g/cm^2 c_B = 938.13g/ cm^2 H = 1200cm	$\text{Tan}\phi_A$ = 0.4245 $\text{Tan}\ \phi_B$ = 0.4245 $3/\gamma H$ =0.001055	F = {$3/\gamma H$ (c_A.X + c_B.Y)} + {(A – ($\gamma_w/2\gamma$).X) }$\tan\phi_A$ + (B – ($\gamma_w/2\gamma$).Y) $\tan\phi_B$ = 0.8055+1.47223-0.1634	F = 1.3057

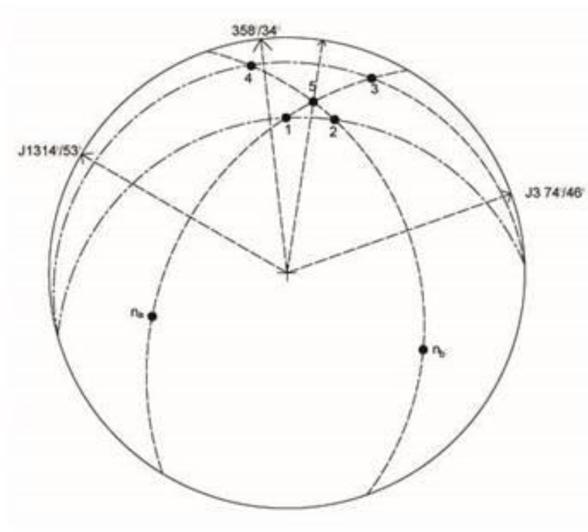

403A/2 J1 - J2

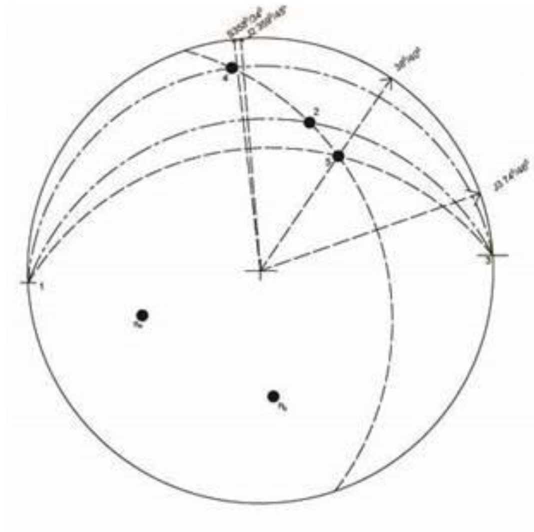

403A/2 J2 – J3

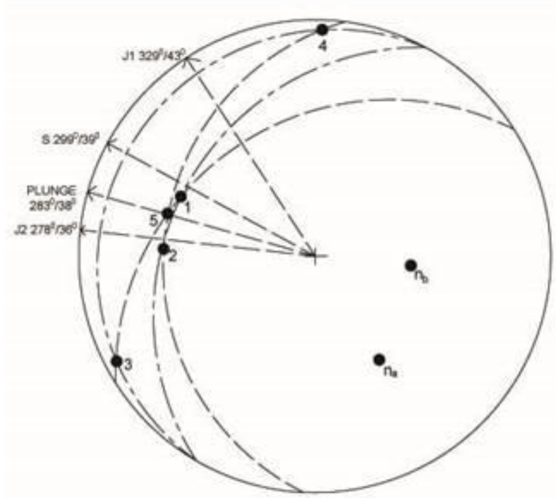

403/2 J1 - J2

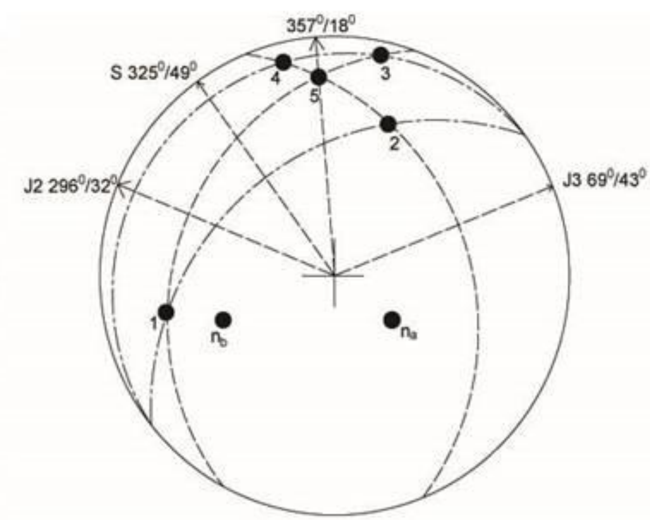

403/5 J2 – J1

Fig 2A. Stereographic projection - Wedge

`